UDC 551.509.313:551.515.2

Numerical Prediction of Tropical Weather Systems

BANNER I. MILLER,[1] PETER P. CHASE, and BRIAN R. JARVINEN[1]—National Hurricane Research Laboratory, Environmental Research Laboratories, NOAA, Miami, Fla.

ABSTRACT—A multilevel primitive-equation model has been designed for regional weather forecasting in the Tropics. Several experimental forecasts have been made on hurricane movement and development and on a nondeveloping tropical weather system. Forecasts of the movement of hurricane Celia were slightly slow and somewhat south of the actual track. Some intensification was forecast as Celia moved into the central Gulf of Mexico, but the model did not predict explosive deepening. Grid spacings of 75 and 150 km were used.

In the nondeveloping case, no deepening was forecast. Areal distribution of the predicted rainfall was good, but the amounts were too light. Forecasts have been made with hand-analyzed input and with interpolated data extracted from the National Meteorological Center's objective analyses.

1. INTRODUCTION

During the past few years, several limited-area, fine-mesh prediction models have been developed for specialized purposes. A few of these are: (1) the 10-level model of Bushby and Timpson (1967), which was designed for the prediction of frontal movement and rainfall; (2) Krishnamurti's model (Krishnamurti 1969, Krishnamurti and Hawkins 1970, Krishnamurti and Moxim 1971), which has been used to predict and study the structure of low-latitude disturbances and mesoscale features of mid-latitude storms; and (3) Miller's (1969) experimental model, developed primarily for the prediction of tropical weather systems, including the formation and movement of hurricanes. Miller's model has been used by Miller and Carlson (1970) to analyze the energetics of an upper tropospheric cold Low in the Tropics, by Rao (1971) to study the lake-induced effects on winter disturbances, and by Carlson (1971) in his analysis of African waves.

The application of limited-area models creates special problems on the lateral boundaries of the forecast domain, and use of small grid spacings in these models can be justified only in areas where data are relatively dense and in locations where special problems (e.g., predicting the point of landfall for a tropical cyclone) require not only a fine-mesh model but also a more complete specification of the physics of the atmosphere. This paper describes the initial attempts to construct such a model. Hemispheric and global models may eventually be able to reduce their grid spacings to the size now being used by the limited-area models, but until the data coverage over the oceans is greatly improved, one might justly question the economic as well as the scientific wisdom of doing so.

2. FORECAST MODEL

The importance of latent heat, sensible heat, and viscous forces in the development and maintenance of tropical weather systems is well known, and a tropical forecast model must obviously include these thermodynamical and mechanical effects. Therefore, a multilevel, diabatic, viscous, primitive-equation model was designed. It has been described in an earlier report (Miller 1969), but the basic framework of the model will be summarized here. The forecast equations (with symbols defined in table 1) are:

$$\frac{\partial u}{\partial t}=-u\frac{\partial u}{\partial x}-v\frac{\partial u}{\partial y}-\omega\frac{\partial u}{\partial p}+fv-\frac{\partial \phi}{\partial x}+K_h\nabla^2 u+g\frac{\partial \tau_x}{\partial p}, \quad (1)$$

$$\frac{\partial v}{\partial t}=-u\frac{\partial v}{\partial x}-v\frac{\partial v}{\partial y}-\omega\frac{\partial v}{\partial p}-fu-\frac{\partial \phi}{\partial y}+K_h\nabla^2 v+g\frac{\partial \tau_y}{\partial p}, \quad (2)$$

$$\frac{\partial \theta}{\partial t}=-u\frac{\partial \theta}{\partial x}-v\frac{\partial \theta}{\partial y}-\omega\frac{\partial \theta}{\partial p}+\frac{\theta}{T}\frac{g}{c_p}\frac{\partial F_s}{\partial p}+\frac{\theta}{T}K_h\nabla^2\theta+\frac{\theta}{c_pT}(H), \quad (3)$$

and

$$\frac{\partial q}{\partial t}=-u\frac{\partial q}{\partial x}-v\frac{\partial q}{\partial y}-\omega\frac{\partial q}{\partial p}+g\frac{\partial F_q}{\partial p}+K_h\nabla^2 q+\frac{dq_s}{dt}. \quad (4)$$

The tangential shearing stresses, τ_x and τ_y, are defined at 1000 mb in terms of the total wind speed, V_0, and the drag coefficient; that is,

$$\tau_{x,0}=-\rho C_d V_0 u \quad (5a)$$

and

$$\tau_{y,0}=-\rho C_d V_0 v. \quad (5b)$$

At the upper levels, these quantities are defined by use of an eddy viscosity for vertical mixing, K_m. They are:

$$\tau_x=-\rho^2 g K_m\frac{\partial u}{\partial p} \quad (6a)$$

and

$$\tau_y=-\rho^2 g K_m\frac{\partial v}{\partial p}. \quad (6b)$$

The fluxes of sensible heat and water vapor at the surface are proportional to the surface wind, the surface

[1] Now at the National Hurricane Center, National Weather Service, NOAA, Coral Gables, Fla.

TABLE 1.—*List of symbols*

C_d	drag coefficient
c_p	specific heat of air at constant pressure
D	divergence
f	Coriolis parameter
f_0	mean value of Coriolis parameter
F_q	flux of water vapor
F_s	flux of sensible heat
g	acceleration of gravity
H	total heating function
H_s	sensible heat (cal · g^{-1} · s^{-1})
HL_1	subsynoptic latent heat (cal · g^{-1} · s^{-1})
HL_2	large-scale latent heat (cal · g^{-1} · s^{-1})
I	net moisture convergence
J	Jacobian operator
K_h	coefficient for lateral mixing
K_m	coefficient for vertical mixing
L	latent heat of condensation
m	map scale factor
p	pressure
p_b	pressure at base of clouds
p_t	pressure at top of clouds
P	precipitation
q	mixing ratio
q_s	saturated mixing ratio
Q	total moisture required to saturate and warm a column
R	gas constant
R_v	gas constant for water vapor
s	distance
T	temperature
T^*	virtual temperature
u	zonal component of the wind
v	meridional component of the wind
V_0	wind speed at the surface
V_r	radial wind speed
$\boldsymbol{V}$	horizontal velocity vector
x	distance in east–west direction
y	distance in north–south direction
α	specific volume
β	$=\frac{df}{dy}$
ζ	relative vorticity
η	absolute vorticity
θ	potential temperature
π	$\equiv\frac{RT}{p\theta}$
ρ	density
σ	static stability, $-\frac{\alpha}{\theta}\frac{\partial\theta}{\partial p}$
τ_x, τ_y	horizontal shearing stresses
ϕ	geopotential, latitude
χ	velocity potential
ψ	stream function
ω	vertical p velocity, $\frac{dp}{dt}$
∇^2	horizontal Laplacian operator

drag coefficient, the air–sea differences in mixing ratio, and temperatures; that is,

$$F_s=\rho_0 C_d c_p(T_w-T_a)V_0 \tag{7a}$$

and

$$F_q=\rho_0 C_d(q_w-q_a)V_0. \tag{7b}$$

These quantities are assumed to decrease linearly with pressure and were allowed to go to zero at 700 mb in the manner suggested by Petterssen et al. (1962); that is, $H_s=g\partial F_s/\partial p$. This technique is consistent with maintaining a quasi-moist adiabatic lapse rate in the lower layers and permits the upward transport of sensible heat against a potential temperature gradient. The surface drag coefficient over water,

$$C_d=(1.0+0.07V_0)\times 10^{-3} \tag{8}$$

is an empirical function of the surface wind speed (Miller 1962, 1964, 1965, 1969, Hawkins and Rubsam 1968) with V_0 being measured in meters per second. Empirical values of K_m and K_h, which were designed to produce realistic values of vertical motion, depth of the inflow layer, and the radial motions in hurricanes (Miller 1965, Barrientos 1964), are also used. It is assumed that K_h, a lateral mixing coefficient, is the same for heat, momentum, and water vapor. Evaporation and the sensible heat over land are set equal to zero and a constant value of 0.005 for the drag coefficient is assumed; this is the value used by Palmén and Holopainen (1962) in their investigation of an extratropical disturbance over the central United States.

The latent heat was computed as the sum of two parts. The first was a parameterization of the subsynoptic scale heating by cumulus convection (Kuo 1965) in which a quantity, Q, is defined as the moisture required to saturate the atmosphere and (following the condensation of a portion of the water vapor) to raise its temperature to that along the moist adiabat passing through the base of the cloud; that is,

$$Q=\int_{p_b}^{p_t}(q_s-q)\frac{\delta p}{g}+\int_{p_b}^{p_t}\frac{c_p}{L}(T_s-T)\frac{\delta p}{g}. \tag{9}$$

By integrating eq (4) in the vertical, we obtain the net moisture covergence within a column,

$$I=\int_{p_b}^{p_t}\frac{\partial q}{\partial t}\frac{\delta p}{g}-\frac{\omega_0 q_0}{g}, \tag{10}$$

where q_0 is the mixing ratio, ω_0 is the vertical motion at 1000 mb, p_b and p_t are the pressures at the base and the top of the clouds, respectively, q_s refers to the saturation mixing ratio, T_s is the temperature along the moist adiabat determined by the lifting condensation level of the subcloud air, and q and T refer to the environmental conditions. The heating function may now be expressed by

$$HL_1=\frac{I}{Q}c_p(T_s-T); \tag{11}$$

$HL_1=0$ at 1000 mb and at 100 mb if $I\leq 0$ or if $T\geq T_s$. Note that the Kuo heating function is self-limiting, since it tends to approach zero as the lapse rate within the cloud becomes moist adiabatic and the cloud becomes saturated.

In the Alma experiment, the convergence of moisture was evaluated by using eq (10). Subsequent work by Miller and Carlson (1970) indicated that the inclusion of the first term in eq (10) contributed little to the total convergence; hence, in the easterly wave and the Celia experiments described in this paper, moisture was assumed to enter the column through the base of the cloud.

The second part of the latent heat release is caused by the ascent of moist air with the broad-scale vertical motion and is defined by

$$HL_2=-c_p\left(\frac{L}{c_p}\frac{\partial q_s}{\partial p}\right)\omega. \tag{12}$$

HL_2 was evaluated when the vertical motion was negative (upward) if the relative humidity was 0.95 or greater. Otherwise, $HL_2=0$; evaporational cooling of falling rain drops was not considered. At temperatures normally prevailing in the Tropics in summer (Jordan 1958), the saturation mixing ratio varies almost linearly with pressure from 700 to 200 mb. With this approximation for $\partial q_s/\partial p$ and an average value of 600 cal/g for L, the quantity enclosed by parentheses in eq (12) has a mean of about 0.06. In the Alma experiment, this constant value was used to speed up the calculations. In the easterly wave and Celia prediction experiments, $\omega(\partial q_s/\partial p)$ was calculated by means of upstream differencing and L was computed as a function of the temperature.

The total heat source, radiation being omitted, is then the sum of the sensible heat, H_s, latent heat released by subsynoptic scales of motion, HL_1 and the latent heat released by large-scale vertical motion, HL_2; that is,

$$H=H_s+HL_1+HL_2. \tag{13}$$

3. BALANCING THE INITIAL DATA

While large-scale motion in the atmosphere is in a quasi-balanced state, complete balance does not and cannot exist, particularly in the presence of large frictional and thermodynamical effects as is the case in tropical cyclones. In addition, observational data contain enough inaccuracies to cause spurious amplification of the natural gravitational and inertial atmospheric oscillations, particularly when the unfiltered forms of the prognostic equations are used in the integration process. To start the forecast, therefore, one should modify the initial data to achieve as nearly a balanced state as can be obtained.

The equations used in our model to achieve this initial balance are the divergence, omega, hydrostatic, continuity, and balance equations. The procedure is similar to that proposed by Charney (1962), Krishnamurti and Baumhefner (1966), and others. The process we use is the following:

1. If winds are available, we solve for the height field using the equation,

$$\frac{\partial D}{\partial t}+\mathbf{V}\cdot\nabla D+\omega\frac{\partial D}{\partial p}+D^2-2J(u,v)-f\zeta+\beta u$$
$$+\frac{\partial\omega}{\partial x}\frac{\partial u}{\partial p}+\frac{\partial\omega}{\partial y}\frac{\partial v}{\partial p}-K_h\nabla^2 D-g\frac{\partial}{\partial p}\left(\frac{\partial\tau_x}{\partial x}+\frac{\partial\tau_y}{\partial y}\right)+\nabla^2\phi=0. \tag{14}$$

Initially, the time-dependent terms are omitted.

If no wind analyses are available, the rotational part of the wind is obtained from the stream function after solving the following equation:

$$f\nabla^2\psi-\beta u+2(\psi_{xx}\psi_{yy}-\psi^2_{xy})=\nabla^2\phi. \tag{15}$$

If winds are available, the stream function is obtained using the expression,

$$\nabla^2\psi=\frac{\partial v}{\partial x}-\frac{\partial u}{\partial y}+u\frac{\tan\phi}{a}, \tag{16}$$

where ϕ is the latitude and a is the radius of the earth.

2. Temperatures are computed from the thicknesses using the hydrostatic equation,

$$\frac{\partial\phi}{\partial p}=-\frac{RT^*}{p}. \tag{17}$$

The computed temperatures are adjusted for moisture as follows:

$$T^*=(1.0+0.6q)\,T. \tag{18}$$

3. The vertical motion is estimated by solving the equation,

$$\nabla^2\sigma\omega+f_0\eta\frac{\partial^2\omega}{\partial p^2}-f_0\omega\frac{\partial^2\eta}{\partial p^2}-f_0\frac{\partial}{\partial p}\left(\frac{\partial\omega}{\partial x}\frac{\partial v}{\partial p}-\frac{\partial\omega}{\partial y}\frac{\partial u}{\partial p}\right)$$
$$=f_0\frac{\partial}{\partial p}(\mathbf{V}\cdot\nabla\eta)-f_0K_h\nabla^2\frac{\partial\eta}{\partial p}-f_0g\frac{\partial^2}{\partial p^2}\left(\frac{\partial\tau_y}{\partial x}-\frac{\partial\tau_x}{\partial y}\right)$$
$$+\pi\nabla^2(\mathbf{V}\cdot\nabla\theta)-\nabla^2\frac{R}{p}(K_h\nabla^2\theta)-\nabla^2\frac{R}{p}\frac{H}{c_p}$$
$$+\pi\nabla^2\frac{\partial\theta}{\partial t}+f_0\frac{\partial}{\partial t}\left(\frac{\partial\eta}{\partial p}\right). \tag{19}$$

At the first pass, the time-dependent terms are omitted. Note that the influence of the vertical diffusion of potential temperature above 700 mb has been omitted from eq (19). This is consistent with the manner in which the vertical flux of sensible heat was treated in eq (3).

4. The total wind is obtained by combining the divergent and the rotational parts of the wind; that is,

$$\nabla^2\chi=-\frac{\partial\omega}{\partial p}, \tag{20}$$

$$u=-\frac{\partial\psi}{\partial y}+\frac{\partial\chi}{\partial x}, \tag{21}$$

and

$$v=\frac{\partial\psi}{\partial x}+\frac{\partial\chi}{\partial y}. \tag{22}$$

5. Temperatures and winds are forecast, and the time-dependent terms in eq (14) and (19) are evaluated from the forecast. Steps 1–5 are repeated several times, usually four or five, until heights and vertical motions are relatively stable.[2]

4. NUMERICAL PROCEDURES AND BOUNDARY CONDITIONS

The finite-difference system developed by Shuman (1962) and now used by the National Meteorological Center (NMC) in the operational primitive-equation forecast model (Shuman and Hovermale 1968) was adopted for these experiments. The details of the finite-difference

[2] Time-dependent terms were not considered in the Alma forecasts.

methods are well known and will not be repeated here. Centered time differences were used after the first step; time steps were 4 min for the 150-km grid and 2 min for the 75-km grid.

In the Alma experiment, the geopotentials on the lateral boundaries were held constant, and the normal component of the wind was assumed to be geostrophic. This procedure resulted in unrealistic gradients of vorticity near the boundaries; these gradients were adjusted periodically by applying a correction so that

$$\oint v_T ds = \oint v_{gT} ds_1 \tag{23}$$

where v_{gT} is the tangential geostrophic wind on the inner boundary, s_1, and v_T is the tangential wind on the outer boundary, s. This adjustment assures that the mean relative vorticity for the forecast domain is equal to the average geostrophic relative vorticity for the area enclosed by the inner boundary.

During the initialization procedure for the other forecasts, boundary heights were held fixed, while eq (14) was solved by relaxation. After convergence had been achieved, the boundary values were calculated by specifying the normal derivatives, $\partial\phi/\partial x$ and $\partial\phi/\partial y$, by use of eq (1) and (2) with frictional, time-dependent, and vertical advective terms being omitted. Equation (14) was solved, and the boundary heights were adjusted a second time before temperatures and vertical motions were computed.

Six data points were used to compute the derivatives needed to adjust the boundary heights. Average values of u, v, f, and the partial derivatives of u and v were defined at the centers of the two boxes adjacent to the row or column for which the boundary height was being computed. These values were then averaged to obtain a mean, which is on a row or a column but midway between the boundary and the second row or column inward from the boundary. Values at the corners of the grid were obtained by averaging the heights at the three adjacent points.

Interior geopotentials were obtained by forming the vertical integral of eq (14) after forecasting u, v, θ, and q. The integrated function was relaxed to obtain a mean geopotential for the seven levels, with mean heights on the boundary being held constant during the relaxation. Heights for the individual levels were then obtained by simultaneous solution of the equations determined by the mean heights and the thicknesses derived by integrating the hydrostatic equation. Boundary heights were recomputed after each 20th time step.

Since the Shuman (1962) finite-difference scheme utilizes nine points, the u and v components of the wind were held constant on the two outer rows during the forecast cycle; the normal and tangential winds were then adjusted on the two outer rows and columns so that the areal means of the divergence and the vorticity for the entire grid were equal to those inside the region where the winds were forecast. To further constrain the amplification of spurious waves near the lateral boundaries, we applied a high lateral viscosity proposed by Benwell and Timpson (1968) to the third and fourth rows and columns in from the boundary. These constraints resulted in stable boundary conditions.

The potential temperature and the mixing ratio were held constant on the boundary at inflow points and were forecast by upstream differencing at outflow points. The vertical motion was set equal to zero on the lateral boundary. Vertical motion at 1000 mb was obtained from the expression,

$$\omega_0 = \frac{\rho g}{f}\left(\frac{\partial}{\partial y} C_d u V_0 - \frac{\partial}{\partial x} C_d v V_0\right), \tag{24}$$

as proposed by Cressman (1963). At 100 mb, the vertical motion was maintained equal to zero to eliminate the external gravity waves. After each time step, the vertical motion was computed from the forecast wind by use of eq (24) and the following:

$$\frac{\partial^2 \omega}{\partial p^2} = -\frac{\partial D}{\partial p}. \tag{25}$$

The use of the second-order form of the equation of continuity does not seem to seriously affect the short-period forecasts of 36–48 hr under most conditions, even though the use of eq (25) does not strictly conserve mass (Peterson 1971, McPherson 1971, Neumann and Mahrer 1971). However, vertical motion tended to become too large in the Alma and Celia forecasts after vorticity centers developed, accompanied by strong low-level inflow. Consequently, the use of eq (25) is not recommended, and any future experiments with our model will place a constraint on the vertically integrated divergence, probably in the manner suggested by O'Brien (1970).

5. RESULTS

Several experimental forecasts have been made with the model. Three examples of these will be described briefly. The first was the Alma experiment, previously discussed in more detail than presented here (Miller 1969). A small geographical area, with a 21 × 21 × 7 array of data points and a grid spacing of about 140 km at 22.5°N, was used. Input data consisting of hand-analyzed winds, mixing ratios, and boundary heights were used. The second example was a nondeveloping wave that caused heavy rainfall over southern Florida in June of 1969. All variables were carried at all seven levels in the vertical. Hand-analyzed winds and mixing ratios were used as initial data. The geographical area was expanded to the area shown in figure 2. An array of 31 × 54 × 7 data points was used. Grid spacing was 153 km at the Equator. The third example was hurricane Celia of August 1970; in this case, height data interpolated from NMC objective analyses were used to obtain the initial wind field by solving the balance equation. Climatological moisture values were used except for the area around the hurricane, where an examination of satellite photographs indicated that saturated values should be used. One forecast was prepared with the 153-km grid spacing and area shown in figure 5A. Another was made with the grid spacing reduced to one-half; that is, about 76.5 km at the Equator.

The Alma Experiment

The disturbance that developed into hurricane Alma in 1962 was tracked for several days before it showed any signs of deepening. By August 26, some deepening had begun off the east coast of Florida. At 1200 GMT on the 27th (fig. 1A), the center was located east of Jacksonville; minimum pressure was about 1006 mb, and highest winds were 20–25 kt just east of the center. The forecast was begun at that time.

At the end of the 24-hr forecast period, the low-level vortex (fig. 1B) had deepened to about 993 mb, and the maximum winds at 1000 mb were slightly in excess of 50 kt. At 850 mb, the strongest winds were more than 60 kt, and the center had moved northward to the North Carolina coast. Comparison with figure 1C shows that the actual movement was somewhat to the right of the forecast track; the vector error was about 60 n.mi.

The advisory issued at 1600 GMT on the 28th stated that the maximum winds were about 52 kt, but later in the afternoon a reconnaissance aircraft reported winds of 80 kt. Other successful portions of the forecast (Miller 1969) indicated the development of an upper level anticyclone and a warming of about 10°C at 250 mb over and to the northeast of the surface center. The maximum inflow was at 1000 mb and the maximum outflow was at 250 mb. The average inflow at 1000 mb at radius of about 4° of latitude was 14 kt, and the average outflow at 250 mb for the same radius was 21 kt. These values are typical for mature hurricanes (Miller 1962, 1964, 1965, Colón 1961). Inflow decreased with height; at 500 mb it was nearly zero, and at 400 mb there was a net outflow at the 4° radius.

The depth of the inflow layer produced by the model appears to be too large, although some data have shown inflow at 500 mb (Colón 1961). The value of K_m was chosen to produce an inflow layer with a depth of about 700 mb (Miller 1965). Also, the use of eq (25) spreads the effects of the friction layer through great depths in a somewhat unrealistic manner. The results of the model suggest that greater vertical resolution, particularly in the lower levels, may be necessary to produce a more realistic inflow layer.

A Nondeveloping Tropical Weather System

During the first week of June 1969, a broad and persistent trough of low pressure extended from southeast of Cape Hatteras, N.C., through central and southern Florida, across Cuba, and into the northwest Caribbean. While quasi-stationary, the trough did oscillate some during the period and caused heavy rains over south Florida. The axis of the wave on the 6th extended from the extreme southeastern Gulf of Mexico to just east of the Yucatán Peninsula (fig. 2). A ridge of high pressure dominated the western portion of the Atlantic, while a smaller anticyclone was over east Texas and the Gulf of Mexico.

Conditions did not appear favorable for tropical storm formation and none developed. A 36-hr forecast beginning with data for 1200 GMT on June 6, 1969, was prepared,

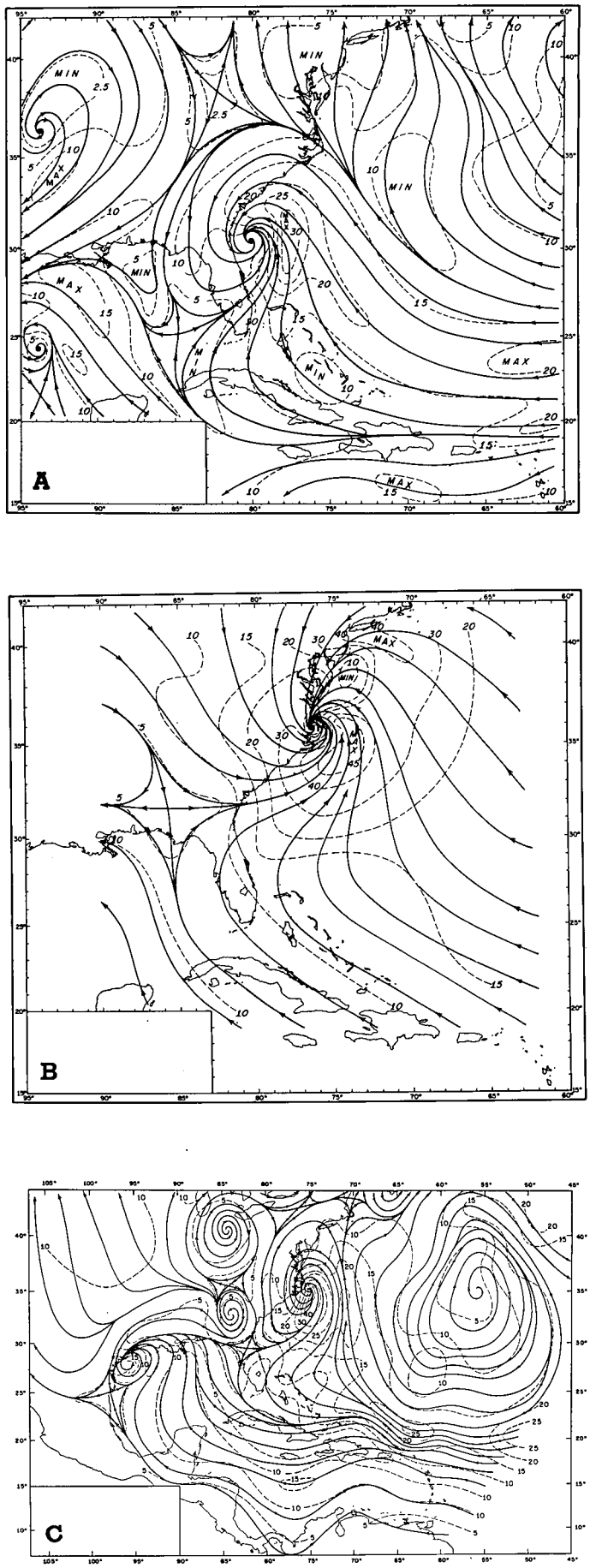

FIGURE 1.—A 1000-mb forecast for hurricane Alma (1962): (A) initial data for 1200 GMT, August 27, (B) 24-hr forecast, and (C) observed wind field for 1200 GMT, August 28.

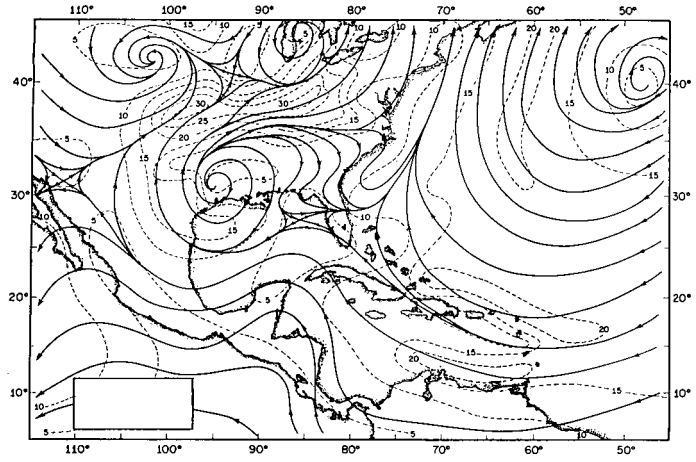

FIGURE 2.—The 1000-mb wind analysis for 1200 GMT, June 6, 1969.

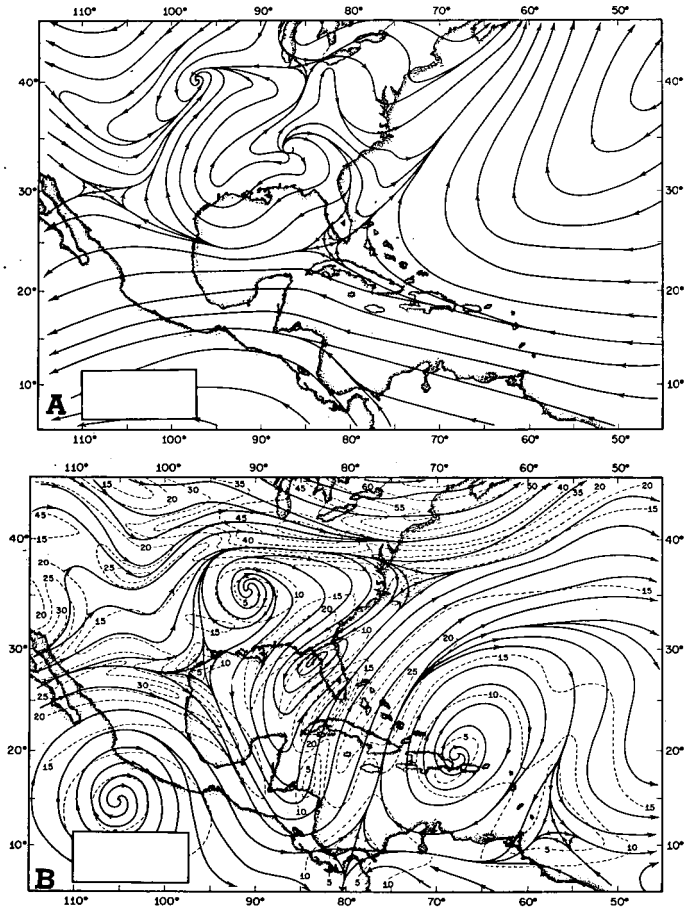

FIGURE 3.—(A) 1000-mb and (B) 500-mb observed data for 1200 GMT, June 7, 1969.

using hand-analyzed winds and mixing ratios as input values.

After 24 hr (fig. 3A), ridging in the western Atlantic continued. The trough in the eastern Gulf of Mexico and western Caribbean had decreased in amplitude, and the flow over Florida had become more northeasterly as the anticyclone over Texas had moved east-northeastward. A general easterly flow persisted over most of the area south of 30°N, with the exception of the weak southwesterly winds in the northern Bahama Islands, which

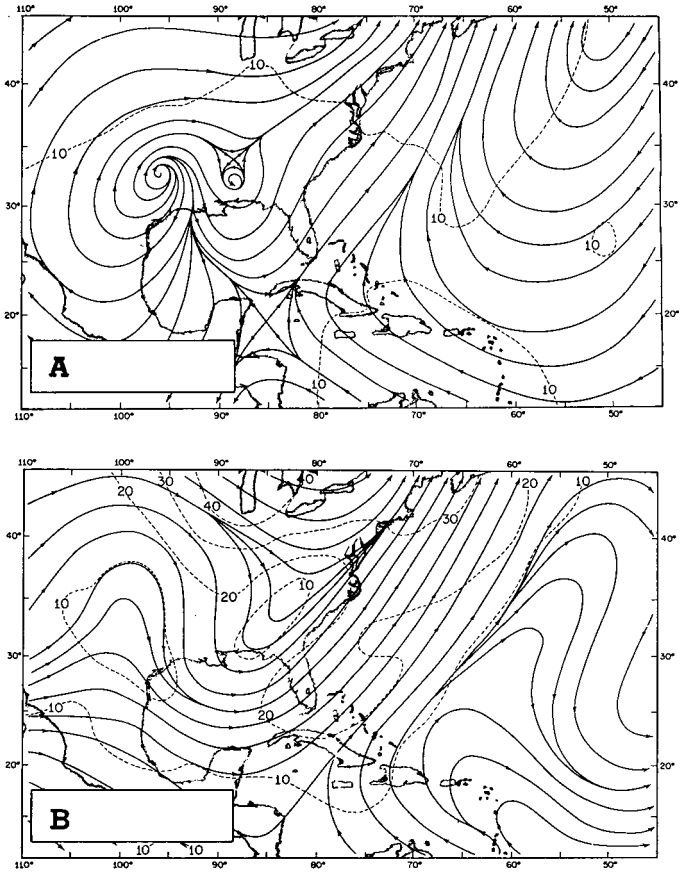

FIGURE 4.—(A) 1000-mb and (B) 550-mb forecasts for 1200 GMT, June 7, 1969.

were just to the east of the trough over extreme south Florida.

The forecast 1000-mb chart (fig. 4A) is generally satisfactory east of about 80°W; the ridge was predicted to remain over the western Atlantic, easterly flow was predicted throughout most of the Caribbean and north of the Lesser Antilles, Puerto Rico, and Hispaniola, southerly winds were forecast over Cuba and the Bahamas. Much of the remainder of the forecast flow is unsatisfactory, as neither the intrusion of the new anticyclone into the forecast domain from outside the boundary nor the resulting movement of the Texas anticyclone toward the east-northeast could be anticipated.

At 550 mb, 24-hr forecast winds over Florida were southerly with speeds greater than 20 kt (fig. 4B). This forecast was approximately correct (fig. 3B). The model maintained more amplitude in the trough over the northeastern United States than actually occurred; the wind speeds were too low (40 kt compared to 55–60 kt) and the motion of the trough was too slow. The forecast also failed to develop a closed Low over the northeastern Gulf of Mexico, and the wave near 100°W was not predicted, since it moved into the forecast area from the western boundary. A ridge was maintained over the western Atlantic, but the small anticyclone north of Hispaniola was not forecast. The low-latitude extension of the east coast trough was predicted, but the amplitude was too small, although the wind speeds were about right. Strong vertical shear over most of the forecast region was maintained.

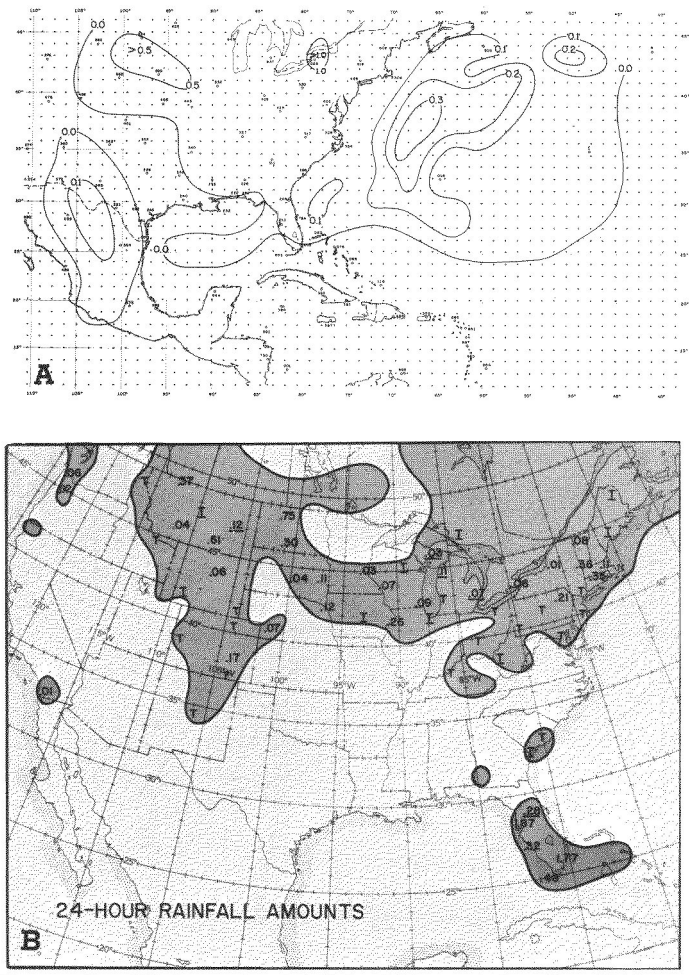

FIGURE 5.—(A) forecast rainfall for 36-hr period ending 0000 GMT, June 8, 1969, and (B) observed rainfall for 24-hr period ending 0600 GMT, June 8, 1969.

The forecast was continued for another 12 hr, mainly to predict rainfall; no major changes in the flow shown in figure 4 were noted (i.e., no tropical storm was predicted to form). Where vertical motion was upward and the relative humidity was 95 percent or greater, rainfall was forecast by

$$P=\int_t^{t+\Delta t}\int_0^{p_0}-\frac{\partial F\omega}{\rho g}\,dpdt, \tag{26}$$

where P is the accumulated precipitation and F, a function defined by Haltiner (1971, p. 164), is

$$F=q_sT\left(\frac{LR-c_pR_vT}{c_pR_vT^2+q_sL^2}\right). \tag{27}$$

Forecast rainfall amounts for the 36-hr period ending 0000 GMT on June 8 are shown in figure 5A, and the 24-hr observed total for June 7 (approx. 0600 GMT, June 7–0600 GMT, June 8) is reproduced in figure 5B.[3] In general, the areal correspondence between the forecast and observed amounts is good, with the main deficiency being over south Florida where predicted amounts were much too light. Over 1 in. of rain fell, but the model forecast 0.10 in. or less; this discrepancy is probably due to the failure of the model to forecast convective rain. No attempt was made to have it do so; this obviously should be corrected.

Elsewhere, general rains were forecast over the northeastern United States, and general rain occurred there. Heaviest amounts were forecast in New York and New England, where about 0.35 in. was recorded in the shorter time period for which data are available. Over 0.5 in. was forecast over the northwestern portion of the grid, and 0.61 in. was recorded at one station slightly to the east of the 0.5 isohyet. This may be fortuitous, since the rainfall there may have been caused by the wave (fig. 3) that moved into the forecast domain from the western boundary.

Forecast for Hurricane Celia of 1970

Hurricane Celia, one of the major storms of recent years, moved into the Gulf of Mexico on Aug. 1, 1970, with a central pressure of 993 mb and highest winds of 70 kt. It deepened during the day to 965 mb, but then the central pressure rose again, and 988 mb was reported on the 3d. Rapid intensification took place as the center approached the Texas coast, and a minimum pressure of 945 mb was reported by a coastal station, representing a deepening of about 26 mb in 9 hr. Highest sustained winds were 105–115 kt, but gusts were estimated to be as high as 140–155 kt.

Two forecasts were prepared for hurricane Celia, beginning with the 1200 GMT, August 2 data which, as stated earlier in the paper, were obtained from NMC height analyses together with climatological moisture values. Saturated moisture values were used in the vicinity of the hurricane. Grid increments of 153 and 76.5 km were used. The winds in figure 6 (Smith 1972) were not used as input for these forecasts, but they are shown as an example of what type of initial data may be derived from surface ships plus satellite winds. Perhaps the inclusion of these winds in the original analyses would have resulted in a better forecast of Celia, but they were not available in real time. Future experiments with this model will attempt to incorporate data of this nature in the initialization process.

After going through the initialization procedure described in section 3, the forecasts were started with a central pressure of about 1007 mb and highest surface winds of 31 kt. On the 153-km grid, intensification was slow. After 12 hr, central pressure had fallen about 4 mb; after 24 hr, minimum pressure was about 998 mb and the highest winds were about 45 kt to the east of the center. The forecast was continued for an additional 12 hr; the center became diffuse and difficult to locate, maximum winds decreased slightly, and the central pressure rose 4 or 5 mb. The track shown in figure 7 was determined by interpolating between gridpoints to obtain the point of minimum pressure; the forecast path was too slow and slightly to the left of the observed movement.

For the second phase of the Celia forecasts, the data on the 153-km grid was converted to a 76.5-km grid, and the data were reinitialized. Development took place more rapidly on the finer grid than on the 153-km grid. After 12

[3] Published rainfall totals were available only on a daily basis (EST); consequently, the forecast and observed periods do not coincide.

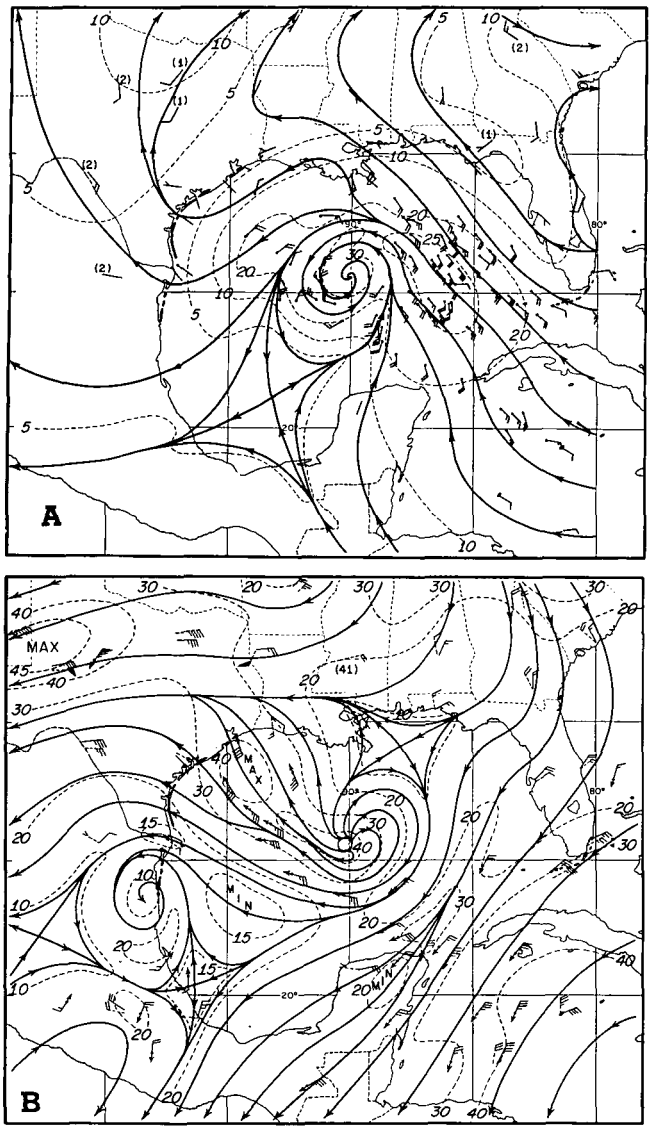

FIGURE 6.—(A) low-level (1200, 1500, 1800, 2100 GMT composite) and (B) high-level (1526–1652 GMT) streamline and isotach (kt) analysis for hurricane Celia, Aug. 2, 1970.

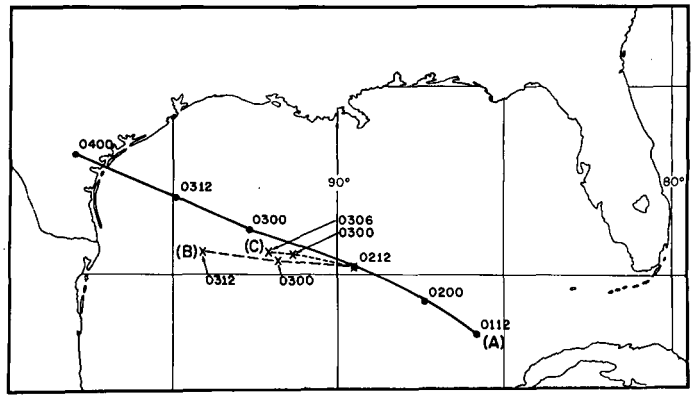

FIGURE 7.—Forecast and observed tracks for hurricane Celia: (A) observed path, (B) 24-hr forecast path on a 153-km grid, and (C) 18-hr forecast track on a 76.5-km grid.

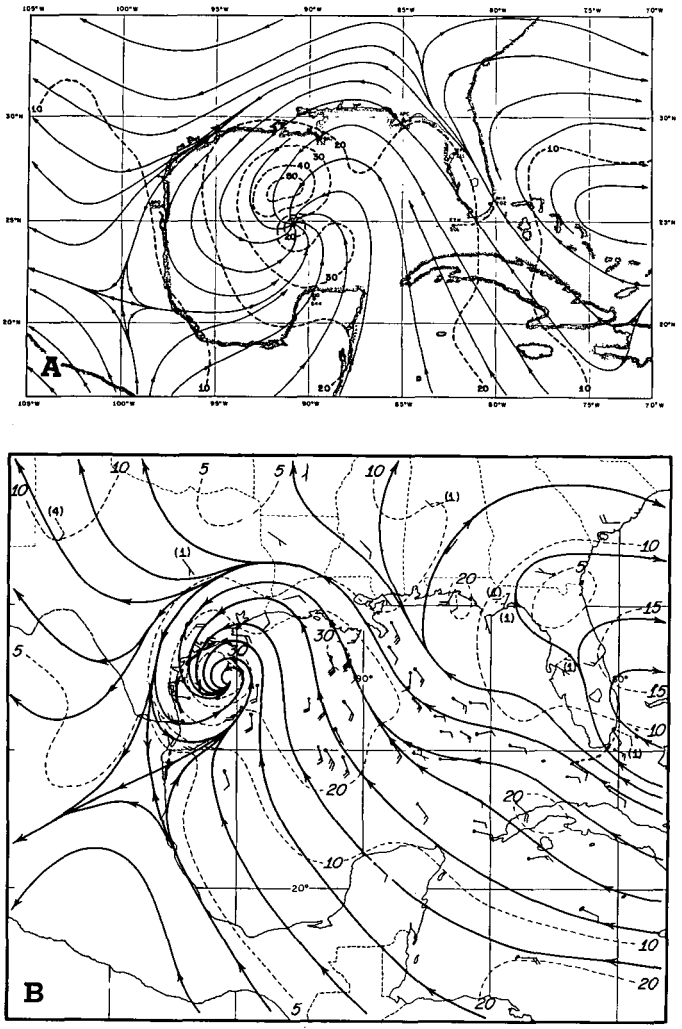

FIGURE 8.—Streamlines and isotachs (kt) for hurricane Celia Aug. 3, 1970: (A) 24-hr forecast of 1000-mb winds for 1200 GMT and (B) observed low-level winds at 1800 GMT.

hr, the central pressure was about 1000 mb and the winds had reached a little more than 40 kt. After 24 hr, predicted surface winds were in excess of 55 kt (fig. 8A); at 250 mb (fig. 9A), winds of more than 45 kt were predicted southwest of the surface center. Comparison between the predicted low-level flow and Smith's surface level composite (fig. 8B) shows some similarities between the two, but the predicted track was again too slow and to the left (fig. 7) of the path. At 250 mb (fig. 9A, 9B), correspondence between forecast and satellite-derived wind analyses was not particularly good, especially concerning the speeds over Texas and the directions over the northwestern Caribbean. The orientation of the isotachs across (rather than along) the streamline southwest of the hurricane center is also not a typically expected feature.

The 1000-mb forecast (fig. 10A) would indicate a surface pressure at the center of about 970 mb. This is a reasonable value, but, as in the Alma experiment, the cyclone is spread out over too large an area, presumably due to the grid spacing (about 75 km) that was used. At 250 mb (fig. 10B), a small thermal anticyclone is present over the surface position of the hurricane. A rise of about 9°C in the 400-mb temperatures was predicted to occur over the developing cyclone (fig. 11).

In figure 12, we have superimposed the predicted vertical motion at 250 mb for 0000 GMT on August 4, which

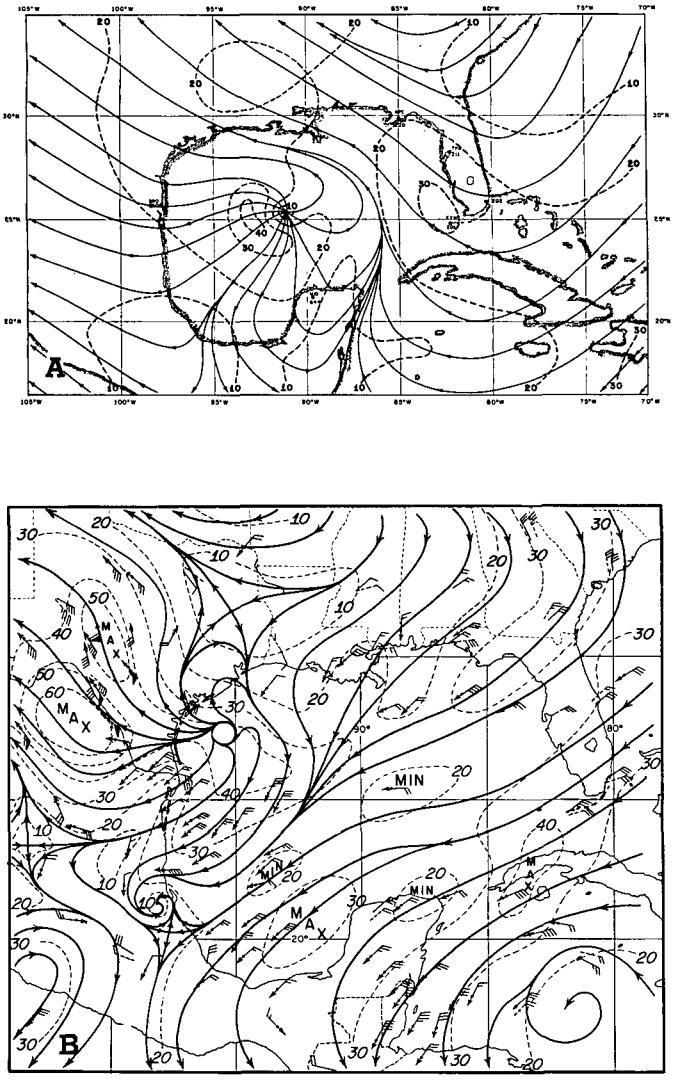

FIGURE 9.—Streamlines and isotachs (kt) for hurricane Celia, Aug. 3, 1970: (A) 24-hr forecast of 250-mb winds for 1200 GMT and (B) observed high-level winds at 1800 GMT.

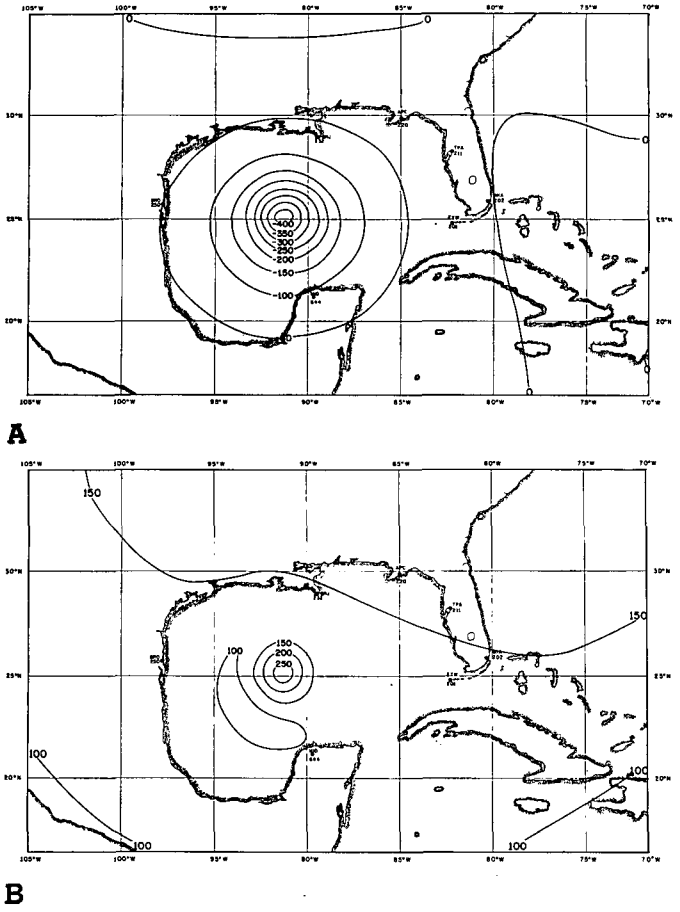

FIGURE 10.—(A) 1000-mb, and (B) 250-mb, 24-hr forecast height anomalies (m) for 1200 GMT, Aug. 3, 1970.

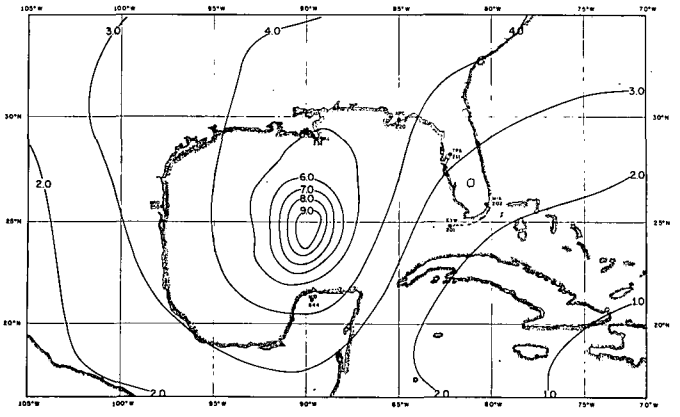

FIGURE 11.—The 400-mb, 24-hr forecast temperature anomalies (°C) for 1200 GMT, Aug. 3, 1970.

is 36 hr after the initial time, on an ATS 3 satellite photograph taken about 6 hr earlier. This forecast was prepared for the 153-km grid. The maximum upward motion was about 5 cm/s over a small area near the center. One would hope for better correspondence between the maximum and the clouds, but, as indicated by figure 7, the predicted movement was too slow and to the left of the actual track. This is indicated by the vertical motion pattern. The model does show a large area of slowly descending air surrounding the cloudy area, as expected.

6. NUMERICAL PROBLEMS

The model described in this report was designed specifically for use in predicting the development and movement of tropical weather systems, in which frictional and diabatic effects play an important role. Therefore, we have tried to make the model as physically realistic as possible. This has led to some problems with the numerics of the model that have not been completely solved.

The method of recovering the geopotential fields following each forecast cycle required the solving of a vertically integrated forcing function by relaxation to obtain the mean heights for the model atmosphere. The required convergence usually took place in less than five scans; if this number became large, it was interpreted as the beginnings of some instability in the computations, the model was programmed to stop, and the data were rebalanced as described in section 3. Rebalancing did not become necessary in the nondeveloping case for a 36-hr forecast. It was required once for the Celia 153-km, 36-hr forecast

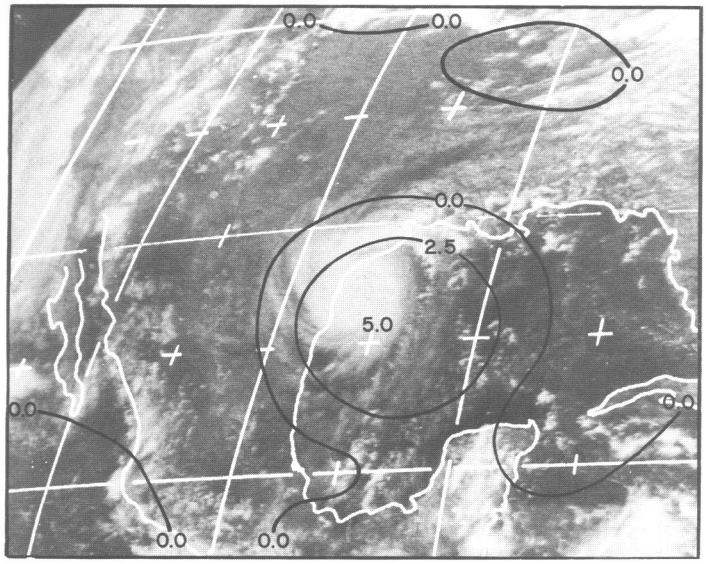

FIGURE 12.—Forecast 250-mb vertical motion (cm/s) for 0000 GMT, Aug. 4, 1970, superimposed on an ATS 3 photograph taken at 1708 GMT, Aug. 3, 1970.

and once for the 75-km, 24-hr forecast. In the Alma experiment, rebalancing was required three or four times, but this can be attributed partly to the small geographical area covered by the forecast domain.

Some of the experiments that were run in an attempt to eliminate the rebalancing included:

1. Omitting the release of latent heat by large-scale vertical motion. No significant cyclone development occurred.

2. Cutting off the large-scale latent heat after a tropical cyclone began to develop a warm core. The incipient hurricane developed a pronounced cold-core Low within 6 hr.

3. Using an "efficiency factor" in application of eq (12); that is, permitting only a fraction of the total latent heat released to go into the warming of the atmosphere. If an efficiency factor of 1.0 were used, rebalancing was required a few hours after precipitation began. A factor of 0.5 permitted the calculations to continue, but the storm moved in a quasi-steady state. A factor of 0.75 permitted a slow increase in the intensity of the storm, but calculations were not extended far enough to determine if this would eliminate rebalancing.

4. The simulated backward difference method as used by Matsuno (1966) was used in lieu of the rebalancing operations. This proved to be less satisfactory and more expensive than repeating the initialization process.

7. SUMMARY

A multilevel baroclinic prediction model, developed primarily for use in tropical regions where data are adequate to justify the use of a fine mesh, has shown some skill in predicting the growth and movement of tropical cyclones. It has also been used to predict the evolution and rainfall associated with a nondeveloping tropical weather system. The model parameterizes subsynoptic scale heating due to cumulus convection and also attempts to calculate the warming of the atmosphere by the release of latent heat through the large-scale vertical motion. Inclusion of this effect appears to be necessary to predict the development of a warm core tropical cyclone.

ACKNOWLEDGMENTS

We would like to thank Clark L. Smith for permission to use some of the illustrations from his paper, R. C. Gentry and Billy M. Lewis for arranging for the necessary computer time to run the experiments, and R. L. Carrodus and his staff for preparing the illustrations. Charles True did the photography. Rita Sherrill, Lorraine Kelly, Shirley Parris, Barbara Creech, and several others assisted in preparing the initial data and in making the calculations. Marcia Wilson typed the manuscript.

REFERENCES

Barrientos, Celso S., "Computations of Transverse Circulation in a Steady State, Symmetric Hurricane," *Journal of Applied Meteorology*, Vol. 3, No. 6, Dec. **1964**, pp. 685–692.

Benwell, G. R. R., and Timpson, Margaret S., "Further Work With the Bushby-Timpson 10-Level Model," *Quarterly Journal of the Royal Meteorological Society*, Vol. 94, No. 399, London, England, Jan. **1968**, pp. 12–24.

Bushby, F. H., and Timpson, Margaret S., "A 10-Level Atmospheric Model and Frontal Rain," *Quarterly Journal of the Royal Meteorological Society*, Vol. 93, No. 395, London, England, Jan. **1967**, pp. 1–17.

Carlson, Toby N., "A Detailed Analysis of Some African Disturbances," *NOAA Technical Memorandum* ERL NHRL–90, U.S. Department of Commerce, National Hurricane Research Laboratory, Miami, Fla., Apr. **1971**, 58 pp.

Charney, Jule G., "Integration of the Primitive Balance Equations," *Proceedings of the International Symposium on Numerical Weather Prediction, Tokyo, Japan, November 7–13, 1960*, Meteorological Society of Japan, Tokyo, Mar. **1962**, pp. 131–152.

Colón, José A., and Staff, "On the Structure of Hurricane Daisy (1958)," *National Hurricane Research Project Report* No. 48, U.S. Department of Commerce, National Hurricane Research Project, Miami, Fla., Oct. **1961**, 102 pp.

Cressman, George P., "A Three-Level Model Suitable for Daily Numerical Forecasting," *Technical Memorandum* No. 22, National Meteorological Center, Washington, D.C., **1963**, 43 pp.

Haltiner, George J., *Numerical Weather Prediction*, John Wiley and Sons, New York, N.Y., **1971**, 317 pp.

Hawkins, Harry F., and Rubsam, Daryl T., "Hurricane Hilda, 1964: Part I. Genesis, as Revealed by Satellite Photographs, Conventional and Aircraft Data," *Monthly Weather Review*, Vol. 96, No. 7, July **1968**, pp. 428–452.

Jordan, Charles L., "Mean Soundings for the West Indies Area," *Journal of Meteorology*, Vol. 15, No. 1, Feb. **1958**, pp. 91–97.

Krishnamurti, T. N., "An Experiment in Numerical Prediction in Equatorial Latitudes," *Quarterly Journal of the Royal Meteorological Society*, Vol. 95, No. 405, London, England, July **1969**, pp. 594–620.

Krishnamurti, T. N., and Baumhefner, David, "Structure of a Tropical Disturbance Based on Solutions of a Multilevel Baroclinic Model," *Journal of Applied Meteorology*, Vol. 5, No. 4, Aug. **1966**, pp. 396–406.

Krishnamurti, T. N., and Hawkins, R. S., "Mid-Tropospheric Cyclones of the Southwest Monsoon," *Journal of Applied Meteorology*, Vol. 9, No. 3, June **1970**, pp. 442–458.

Krishnamurti, T. N., and Moxim, Walter J., "On Parameterization of Convective and Nonconvective Latent Heat Release," *Journal of Applied Meteorology*, Vol. 10, No. 1, Feb. **1971**, pp. 3–13.

Kuo, H. L., "On Formation and Intensification of Tropical Cyclones Through Latent Heat Release by Cumulus Convection," *Journal of the Atmospheric Sciences*, Vol. 22, No. 1, Jan. **1965**, pp. 40–63.

Matsuno, Taroh, "Numerical Integrations of the Primitive Equations by a Simulated Backward Difference Method," *Journal of the Meteorological Society of Japan*, Ser. 2, Vol. 44, No. 1, Tokyo, Feb. **1966**, pp. 76–84.

McPherson, Ronald D., "Reply," *Journal of Applied Meteorology*, Vol. 10, No. 3, June **1971**, pp. 600–601.

Miller, Banner I., "On the Momentum and Energy Balance of Hurricane Helene (1958)," *National Hurricane Research Project Report* No. 53, U.S. Department of Commerce, National Hurricane Research Project, Miami, Fla., Apr. **1962**, 19 pp.

Miller, Banner I., "A Study of the Filling of Hurricane Donna (1960) Over Land," *Monthly Weather Review*, Vol. 92, No. 9, Sept. **1964**, pp. 389–406.

Miller, Banner I., "A Simple Model of the Hurricane Inflow Layer," *National Hurricane Research Laboratory Report* No 75, U.S. Department of Commerce, National Hurricane Research Laboratory, Miami, Fla., Nov. **1965**, 16 pp.

Miller, Banner I., "Experiment in Forecasting Hurricane Development With Real Data," *ESSA Technical Memorandum* ERLTM–NHRL 85, U.S. Department of Commerce, National Hurricane Research Laboratory, Miami, Fla., Apr. **1969**, 28 pp.

Miller, Banner I., and Carlson, Toby N., "Vertical Motions and the Kinetic Energy Balance of a Cold Low," *Monthly Weather Review*, Vol. 98, No. 5, May **1970**, pp. 363–374.

Neumann, J., and Mahrer, Y., "A Theoretical Study of the Land and Sea Breeze Circulation," *Journal of the Atmospheric Sciences*, Vol. 28, No. 4, May **1971**, pp. 532–542.

O'Brien, James J., "Alternative Solutions to the Classical Vertical Velocity Problem," *Journal of Applied Meteorology*, Vol. 9, No. 2, Apr. **1970**, pp. 197–203.

Palmén, Erik, and Holopainen, E. O., "Divergence, Vertical Velocity and Conversion Between Potential and Kinetic Energy in an Extratropical Disturbance," *Geophysica*, Vol. 8, No. 2, Geophysical Society of Finland, Helsinki, **1962**, pp. 89–112.

Peterson, Ernest W., "Comments on 'A Numerical Study of the Effect of a Coastal Irregularity on the Sea Breeze,' " *Journal of Applied Meteorology*, Vol. 10, No. 3, June **1971**, pp. 599–600.

Petterssen, Sverre, Bradbury, Dorothy L., and Pedersen, Kaare, "The Norwegian Cyclone Models in Relation to Heat and Cold Sources," *Geofysiske Publikasjoner*, Vol. 24, No. 9, Det Norske Videnskaps-Akademi I, Oslo, Norway, Feb. **1962**. pp. 243–280.

Rao, Gandikota V., "Some Mesoscale Features of the Initial Fields of Motion and Temperature for a Lake-Induced Winter Disturbance," *Journal of Applied Meteorology*, Vol. 10, No. 4, Aug. **1971**, pp. 694–702.

Shuman, Frederick G., "Numerical Experiments With the Primitive Equations," *Proceedings of the International Symposium on Numerical Weather Prediction, Tokyo, Japan, November 7–13, 1960*, Meteorological Society of Japan, Tokyo, Mar. **1962**, pp. 85–107.

Shuman, Frederick G., and Hovermale, John B., "An Operational Six-Layer Primitive Equation Model," *Journal of Applied Meteorology*, Vol. 7, No. 4, Aug. **1968**, pp. 525–547.

Smith, Clark L., "On the Intensification of Hurricane Celia, 1970," National Hurricane Research Laboratory, Miami, Fla., Mar. **1972**, 57 pp. (personal communication).

[*Received February 28, 1972; revised June 30, 1972*]